

A Magnetic Model for the Ordered Double Perovskites

Prabuddha Sanyal and Pinaki Majumdar

Harish-Chandra Research Institute, Chhatnag Road, Jhusi, Allahabad 211019, India

(Dated: Dec 5, 2008)

We construct an effective spin model from the coupled spin-fermion problem appropriate to double perovskites of the form $A_2BB'O_6$. The magnetic model that emerges is reminiscent of double exchange and we illustrate this ‘reduction’ in detail for the case of perfect B-B’ structural order, i.e, no antisite disorder. We estimate the effective exchange between the magnetic B ions in terms of the electronic parameters, study the ‘classical’ magnetic model using Monte Carlo techniques, and compare this approach to a full numerical solution of the spin-fermion problem. The agreement is reasonable, and promises a quick estimate of magnetic properties when coupled with *ab initio* electronic structure. The scheme generalises to the presence of antisite disorder.

I. INTRODUCTION

Double perovskite materials, of the form $A_2BB'O_6$, have been of interest in recent years^{1,2} on account of their magnetic, electronic and structural properties. They promise large magnetoresistance^{3,4,5}, potentially useful for switching applications. The half-metallic character of some of the members also make them attractive candidates for spintronic devices.

One of the species, B say, is typically magnetic, a transition metal like Fe, Co, Ni, or Cr, while the B’ species is generally non-magnetic, Mo, W, *etc.* The most studied member of this series is Sr_2FeMoO_6 : it is a half-metallic ferromagnet (FM) at low temperature, and has a high $T_c \sim 410K$. Sr_2FeWO_6 , on the other hand, is an anti-ferromagnetic (AFM) insulator! These limits illustrate the wide range of physical properties in the double perovskites (DP). While the ‘endpoints’ above are relatively easy to understand (ignoring disorder) there are several effects where current understanding is limited.

(i) *Antisite disorder*: Well annealed double perovskites tend to have an alternate arrangement of B and B’ ions, but defects called ‘antisite’ regions⁶ appear when two B or two B’ atoms occur as neighbours. These regions typically have an AFM arrangement of the B spins and are insulating. Their presence reduces the overall magnetization. The electronic and magnetic properties in DP’s are intimately related to the structural order.

(ii) *Phase competition*: Exploration of the series^{7,8} $Sr_2FeMo_{1-x}W_xO_6$ reveals a FM to AFM transition and an associated metal-insulator transition (MIT) with increasing x . In the regime of FM-AFM phase competition the compounds show large magnetoresistance (MR).

(iii) *Magnetic B’ sites*: Recently, compounds where the B’ site also has an intrinsic magnetic moment have been investigated⁹, and interesting compensation effects have been observed. In particular, there are enigmatic compounds like Sr_2CrOsO_6 which are insulating (semimetallic?), but at the same time ferromagnetic, with a very high T_c ¹⁰. In addition, there are spin-orbit effects¹¹ in some DP’s complicating the magnetic state.

Approaching issues (i)-(iii) above directly in a finite temperature real space formulation is formidable. It re-

quires tools that can predict magnetic properties of a double perovskite based on electronic parameters and the structural disorder. This paper is a step towards that goal where we provide a semi-analytic scheme for accessing the magnetic ground state and T_c scales of a structurally ordered DP starting with a tight-binding spin-fermion model. While our primary focus is the FM regime, we also highlight issues of phase competition and antiferromagnetism which are bound to be important when doping effects are explored.

The paper is organised as follows. The next section describes the double perovskite model, following which we summarise earlier work on this problem to place our work in context. We then outline the different methods used in this study. The section after describes our results, primarily within a variational scheme and an effective exchange calculation, with Monte Carlo results for benchmark. We then conclude, pointing out how our scheme can be extended to the antisite disordered case.

II. THE DOUBLE PEROVSKITE MODEL

The double perovskite structure of $A_2BB'O_6$ can be viewed as repetition of the perovskite units ABO_3 and $AB'O_3$. In the ideal ordered DP the B and B’ octahedra alternate in each direction. In this paper we consider only the B ion to be magnetic. The superexchange coupling between the B magnetic moments is small in the ordered DP’s. The important physical ingredients in the problem are: (i) a large S core spin at the B site, (ii) strong coupling on the B site between the core spin and the itinerant electron, strongly preferring *one* spin polarisation of the itinerant electron, and (iii) delocalisation of the itinerant electron on the B-O-B’ network.

The Hamiltonian for the structurally (B-B’) ordered double perovskites is given by:

$$H = \epsilon_B \sum_{i \in B} f_{i\sigma}^\dagger f_{i\sigma} + \epsilon_{B'} \sum_{i \in B'} m_{i\sigma}^\dagger m_{i\sigma} - \mu \sum_i (n_{f,i} + n_{m,i}) - t \sum_{\langle ij \rangle \sigma} f_{i\sigma}^\dagger m_{j\sigma} + J \sum_{i \in A} \mathbf{S}_i \cdot f_{i\alpha}^\dagger \vec{\sigma}_{\alpha\beta} f_{i\beta} \quad (1)$$

The f ’s refer to the magnetic B sites and the m to the non

magnetic B', and the B-B' hopping $t_{BB'} = t$ is the principal hopping in the structurally ordered DP's. We will discuss the impact of further neighbour hoppings later in the text. We have retained only one orbital on the B and B' site, our formulation readily generalises to a multiple orbital situation. The \mathbf{S}_i are 'classical' (large S) core spins at the B site, coupled to the itinerant B electrons through a coupling $J \gg t$. This implies that the conduction electron state at a B site is slaved to the orientation of the corresponding B spin. The difference between the ionic levels, $\Delta = \epsilon_B - \epsilon_{B'}$, defines the 'bare' 'charge transfer' energy. At a later stage we will define the parameter $\Delta = (\epsilon_B - JS/2) - \epsilon_{B'}$ as the 'true' charge transfer energy. n_f is the B electron occupation number, while n_m is the B' electron occupation number. We will assume $J/t \rightarrow \infty$ (keeping Δ finite). The parameter space of the problem is defined by the electron filling, n , the ratio Δ/t and the temperature T/t . We have ignored Hubbard repulsion, B-B antiferromagnetic superexchange, and, to start with, direct hopping between B'-B', or B-B.

III. EARLIER WORK

Early work on the DP's was motivated by results on $\text{Sr}_2\text{FeMoO}_6$, where electronic structure calculations indicate that Fe is in a $3d^5$ configuration (a half-filled state) while Mo is in a $4d^1$ configuration. Following Hund's rule, Fe is therefore in a high spin $S = 5/2$ state. Surprisingly, the normally nonmagnetic Mo picks up a moment of $1/2$ in the opposite direction, and reduces the moment per unit cell to $\sim 4\mu_B$. An explanation for the induced moment on the non magnetic B' species was provided¹² by Sarma *et al.*, in terms of a 'level repulsion' between the Fe and Mo levels. Such a scenario implies a substantial degree of hybridization between the Fe and Mo orbitals, and assumes that the itinerant Mo electron hops through the Fe sublattice.

Using this idea, a double-exchange (DE) like 2-sublattice Kondo lattice model was proposed for the DP's¹³, and solved within dynamical mean field theory by Chattopadhyay and Millis¹³, assuming a 'ferrimagnetic'¹⁴ state. They obtained a $n - T$ phase diagram for different values of $\epsilon_{B'} - \epsilon_B$ and J and observed that the T_c goes to zero at large filling, indicating the presence of some competing non ferromagnetic state.

A similar result for $T_c(n)$ was obtained by Carvajal *et al.*¹⁵ using another two sublattice model, and Ising spins. Here the hopping of an electron with spin σ from a B' site to a neighbouring B site is t if σ is antiparallel to the local spin μ_i on that site, while it is zero if they are parallel. The authors considered only ferrimagnetic arrangements.

Alonso *et al.*¹⁶ considered a variant of Millis' model with the coupling $J \rightarrow \infty$, but with a larger number of ordering possibilities. They also took into account possible antisite defects, including a B-B hopping and superexchange which are only active when two B atoms become nearest neighbours. They considered four possi-

ble phases: (1) paramagnetic, (2) ferrimagnetic, (3) an AFM phase, where the B spins in neighbouring (1,1,1) planes are antiparallel, and (4) another ferrimagnetic phase where the B spins are aligned ferromagnetically if the B are in the correct positions, and antiferromagnetically if the B ions occupy B' sites due to antisite defects. Among other results they found that even in the B-B' ordered case (where superexchange is not operative) the AFM phase is preferred to the FM at high band filling.

All these studies, except the paper by Alonso *et al.*, concentrate on the ferromagnetic¹⁴ phase. They observe the decrease of T_c at large filling but do not explore competing phases. Secondly, while the DMFT approaches provide a semianalytic treatment of the T_c scales, in specific parts (in this case ferromagnetic) of the phase diagram, an estimate of the effective exchange between the B moments is not available. The *ab initio* approaches have attempted such an estimate by force fitting a 'Heisenberg model'. Unfortunately, the magnetic states that emerge from the DP model, and the effective exchange that stabilises these phases arise from subtle electron delocalisation physics not captured by such methods. We also do not know of any work that allows an economical and systematic exploration of the parameter space, n , Δ , J , of the DP model. The present paper aims to overcome these shortcomings.

IV. METHODS

The first estimate of magnetic interactions in any material is provided by *ab initio* calculations. This is typically done by calculating the difference in ground state energy of the compound in spin polarized and spin-unpolarized configurations; or in different magnetic ground states corresponding to different values of the spin density wave vector¹². Such a calculation involves all the relevant orbitals and their hybridization and provides a rough material specific estimate. However, for complex antiferromagnetic ground states one has to guess such configuration beforehand, or take a cue from experiments. There is no *a-priori* prescription for finding them.

Model Hamiltonian based calculations, on the other hand, have the obvious limitation that model parameters have to be inferred from elsewhere, typically *ab initio* studies^{18,19}. The advantage, however, lies in the simplicity of the resulting model, and our ability to create a qualitative understanding using the tools of statistical mechanics. The Hamiltonian appropriate to double perovskites can be studied using the following tools: (i) a combination of exact diagonalization and Monte Carlo (ED-MC), (ii) variational calculation (VC) based on some family of periodic spin configurations, and (iii) mapping to an effective classical spin model.

The ED-MC approach has the advantage of accessing the magnetic structure without bias. However, due to large computational cost, it is severely size-limited, limit-

ing the class of magnetic structures which can be probed. A ‘travelling cluster’ (TCA) variant²⁵ of ED-MC allows use of somewhat larger system size. Variational calculations assuming a periodic spin background can be used for very large system size (since there is no bulk diagonalisation needed) but are restricted by the choice of the variational family. While we will use both (i) and (ii) above, our principal tool will be (iii), where we map on the spin-fermion problem to an effective spin only model, with exchange calculated from the fermions²⁶. We describe (i)-(iii) in more detail below.

A. Monte Carlo

One can solve the DP model on a finite lattice by direct numerical methods, allowing for an ‘exact’ benchmark for approximate solutions. ED-MC is such a technique. Here, the coupled spin-fermion problem is solved by updating the classical spins using a Monte Carlo, diagonalizing the fermion system at each step of the MC to infer the energy cost of the move. The method is numerically expensive and can only be used on small system sizes, $\sim 8 \times 8$. Substantially bigger sizes, $\sim 24 \times 24$, can be accessed using the TCA.

For the MC implementation the Hamiltonian of Eq 1 has to be cast into form appropriate for $J \rightarrow \infty$. This is done by performing a rotation to the local \mathbf{S}_i axis at each B site, and retaining only the electron state oriented antiparallel to \mathbf{S}_i at that site. This gives the following Hamiltonian, with ‘spinless’ B conduction electrons and B’ electrons having both spin states.

$$H = t \sum_{\langle ij \rangle} \left\{ \left(\sin\left(\frac{\theta_i}{2}\right) f_i^\dagger m_{j\uparrow} - e^{i\phi_i} \cos\left(\frac{\theta_i}{2}\right) f_i^\dagger m_{j\downarrow} \right) + h.c. \right\} + \epsilon_B \sum_i f_i^\dagger f_i + \epsilon_{B'} \sum_{i\sigma} m_{i\sigma}^\dagger m_{i\sigma} \quad (2)$$

There is no longer any ‘infinite’ coupling in the model, and the number of degrees of freedom has been reduced to one per B site (and 2 per B’), so the Hilbert space is a little smaller. $m_{j\downarrow}$ and $m_{j\uparrow}$ hop to different conduction electron projections at the neighbouring B site(s) so the effective hopping picks up a θ_i, ϕ_i dependent modulation. We will use this form of the DP model for the Monte Carlo.

B. Variational ground state

A more analytical method used before in the double exchange context is to write down a family of spin configurations $\{\mathbf{S}\}_\alpha$, denoted S_α for simplicity, and calculate the electronic energy in that background. Since the S_α are usually periodic this is effectively a ‘band structure’ calculation. For a specified chemical potential one can calculate the electronic energy $\mathcal{E}(\mu, S_\alpha)$. The configuration $S_{min}(\mu)$ that minimises \mathcal{E} is the variational ground

state. Needless to say, the ‘minimum’ is only as good as the starting set, and in general non periodic S_α cannot be handled. Nevertheless, used in combination with MC results it can be a valuable tool.

From the MC we will discover that in the structurally ordered case the DP model has simple periodic ground states, with windows of phase separation in between. This will allow us to use the variational scheme, with only a few configurations, to map out the $T = 0$ phase diagram accurately.

C. Effective exchange

The complications with spin-fermion MC, and the limitations of VC could be avoided if one had an explicit spin-spin interaction model deduced from the starting DP model. Formally such a scheme can be written down, and some progress made through approximation. Let us illustrate this ‘self consistent renormalisation’ (SCR) principle²⁶ in the simpler context of double exchange before moving to the double perovskites.

1. Illustrative case: double exchange model

Consider the following model:

$$H = \sum_{ij\sigma} t_{ij} c_{i\sigma}^\dagger c_{j\sigma} - J \sum_{i,\alpha\beta} \mathbf{S}_i \cdot c_{i\alpha}^\dagger \vec{\sigma}_{\alpha\beta} c_{i\beta} \quad (3)$$

Let us try to construct an approximate classical spin model in the limit $J \rightarrow \infty$. The classical model is defined by the equivalence:

$$\int \mathcal{D}\mathbf{S}_i e^{-\beta H_{eff}\{\mathbf{S}\}} = \int \mathcal{D}\mathbf{S}_i \text{Tr} e^{-\beta H} \quad (4)$$

where the trace is over the fermion degrees of freedom. The trace, in general, is impossible to compute analytically since it involves the spectrum of fermions moving in an *arbitrary* spin background $\{\mathbf{S}\}$. Nevertheless, some headway can be made once the Hamiltonian is written in a more suggestive rotated and projected basis as²⁶:

$$H = \sum_{ij} f_{ij} t_{ij} (e^{i\Phi_{ij}} \gamma_i^\dagger \gamma_j + h.c.) \quad (5)$$

where $f_{ij} = \sqrt{\frac{1+\mathbf{S}_i \cdot \mathbf{S}_j}{2}}$, Φ_{ij} is a phase factor depending on \mathbf{S}_i and \mathbf{S}_j , and the γ are ‘spinless’ fermion operators. This suggests the approximation:

$$H_{eff}\{\mathbf{S}\} \approx - \sum_{ij} D_{ij} \sqrt{\frac{1+\mathbf{S}_i \cdot \mathbf{S}_j}{2}} D_{ij} = -t_{ij} \langle \langle e^{i\Phi_{ij}} \gamma_i^\dagger \gamma_j + h.c. \rangle \rangle \quad (6)$$

The angular brackets indicate first a quantum average (for fixed $\{\mathbf{S}\}$) and then thermal average over $e^{-\beta H_{eff}\{\mathbf{S}\}}$.

Another way to obtain the same result, which generalises to the DP problem, is to write the action for H in a spin background $\{\mathbf{S}\}$:

$$\mathcal{A}\{\mathbf{S}\} = \beta \sum_{n,i,j} [\dot{\omega}_n \delta_{ij} - t_{ij} f_{ij} e^{i\Phi_{ij}}] \gamma_{in}^\dagger \gamma_{jn} \quad (7)$$

and the internal energy $U\{\mathbf{S}\} = \frac{\partial \ln Z\{\mathbf{S}\}}{\partial \beta} = -\langle \frac{\partial \mathcal{A}}{\partial \beta} \rangle$;

$$\begin{aligned} U\{\mathbf{S}\} &= \sum_{ij} f_{ij} t_{ij} e^{i\Phi_{ij}} \sum_n \langle \gamma_{in}^\dagger \gamma_{jn} \rangle \\ &= \sum_{ij} f_{ij} t_{ij} (e^{i\Phi_{ij}} \langle \gamma_i^\dagger \gamma_j \rangle + h.c.) \end{aligned} \quad (8)$$

which is simply the quantum average of the spin-fermion Hamiltonian for a fixed $\{\mathbf{S}\}$. As before we can convert this to an approximate spin Hamiltonian by thermally averaging the quantity within the round brackets.

The effective exchange depends on T , but in the ‘clean’ problem it does not depend on the ‘bond’ ij . Since the DE model always has a ferromagnetic ground state, the low T exchange can be calculated from the fermionic average in the *fully polarised* state, and is simply:

$$D \propto \sum_k \epsilon_k \langle n_k \rangle = \sum_k \epsilon_k n_F(\epsilon_k)$$

It was observed²⁶ that even at finite temperature the *self consistent average* in the ferromagnetic phase remains close to the $T = 0$ value till very near T_c . The $T = 0$ kinetic energy therefore provides a reasonable estimate of effective ferromagnetic exchange, and so the T_c . The overall scale factor between the T_c and the exchange can be determined from a Monte Carlo calculation.

2. Effective exchange in the double perovskites

Unlike the DE model we cannot write an effective spin only Hamiltonian for the double perovskites purely by inspection since the electron motion also involves the B’ sites. We use the action formulation instead. Integrating out the B’ electrons we get an action entirely in terms of the B degrees of freedom:

$$\begin{aligned} \mathcal{A}\{\mathbf{S}\} &= \beta \sum_n \left(\sum_{k\sigma} f_{kn\sigma}^\dagger G_{ff0}^{-1}(k, i\omega_n) f_{kn\sigma} \right. \\ &\quad \left. - J \sum_i \mathbf{S}_i \cdot f_{in\mu}^\dagger \vec{\sigma}_{\mu\nu} f_{in\nu} \right) \end{aligned} \quad (9)$$

where $G_{ff0}(k, i\omega_n)$ is the $J = 0$ Greens function involving B sites only (the n represent Matsubara frequencies):

$$G_{ff0}^{-1} = i\omega_n - (\epsilon_B - \mu) - \frac{\epsilon_k^2}{i\omega_n - (\epsilon_{B'} - \mu)} \quad (10)$$

If we choose $\epsilon_B = 0$, $\epsilon_{B'} = \Delta < 0$, this becomes:

$$G_{ff0}^{-1} = i\omega_n + \mu - \frac{\epsilon_k^2}{i\omega_n + \mu - \Delta} \quad (11)$$

where $\epsilon_k = 2t \sum_{i=1}^d \cos k_i a$. The poles of this Greens function give the band dispersion at $J = 0$:

$$E_k^\pm = \frac{\Delta \pm \sqrt{\Delta^2 + 4\epsilon_k^2}}{2} - \mu \quad (12)$$

In the limit $\Delta \gg t$, i.e., the limit of weak charge transfer, there are two bands centred roughly on 0 and Δ . For $\Delta = 0$, there are two bands $\pm |\epsilon_k|$ symmetrically placed about 0.

While the first term in the action involving this bare Greens function conserves spin and momentum, the second term is local in real space and typically involves spin-flip. To proceed, let us Fourier transform $G_{ff0}^{-1}(k, \omega)$ and write the action in real space. ϵ_k^2 generates ‘hoppings’ (in the full B-B’ lattice) connecting sites that can either be next nearest neighbours (2N), next-to next nearest neighbours (3N), or the same site. In real space the action assumes the form:

$$\begin{aligned} \mathcal{A}\{\mathbf{S}\} &= \beta \sum_n \left(\sum_{ij\sigma} f_{in\sigma}^\dagger G_{ff0}^{-1}(\vec{r}_i - \vec{r}_j, i\omega_n) f_{jn\sigma} \right. \\ &\quad \left. - J \sum_i \mathbf{S}_i \cdot f_{in\alpha}^\dagger \vec{\sigma}_{\alpha\beta} f_{in\beta} \right) \end{aligned} \quad (13)$$

Now, an unitary transformation is performed in spin space so that the second term in the action becomes diagonal: $\gamma_{in\mu} = \sum_\alpha A_{\mu\alpha}^i f_{in\alpha}$. The action becomes:

$$\begin{aligned} \mathcal{A}\{\mathbf{S}\} &= \beta \sum_n \left(\sum_{ij\mu,\nu\sigma} g_{\mu\nu}^{ij} \gamma_{i\mu n}^\dagger G_{ff0}^{-1}(\vec{r}_i - \vec{r}_j, i\omega_n) \gamma_{j\nu n} \right. \\ &\quad \left. - \frac{JS}{2} \sum_i (\gamma_{i\mu n}^\dagger \gamma_{i\mu n} - \gamma_{i\nu n}^\dagger \gamma_{i\nu n}) \right) \end{aligned} \quad (14)$$

where $g_{\mu\nu}^{ij} = \sum_\sigma A_{\mu\sigma}^i A_{\sigma\nu}^j$.

At large J one projects out the γ_{iu} states, retaining only the terms involving the index l . Thereafter, we drop this index, redefine the B level as $\epsilon_B \rightarrow \epsilon_B - \frac{JS}{2}$, and obtain an effective spinless fermion model similar to the case of double exchange.

$$\begin{aligned} \mathcal{A}\{\mathbf{S}\} &= \beta \sum_{ij} g_{ij} \bar{\gamma}_{in} G_{ff0}^{-1}(\vec{r}_i - \vec{r}_j, i\omega_n) \gamma_{jn} \\ &= \beta \sum_{ij} g_{ij} \left((i\omega_n + \mu) \delta_{ij} - \frac{h_{ij}}{i\omega_n + \mu - \Delta} \right) \bar{\gamma}_{in} \gamma_{jn} \end{aligned}$$

where $g_{ij} = \sqrt{\frac{1+\mathbf{S}_i \cdot \mathbf{S}_j}{2}} e^{i\Phi_{ij}}$ as before. h_{ij} is the Fourier transform of ϵ_k^2 and connects sites on the B sublattice. It involves a NN term ($\hat{x} + \hat{y}$ in the full B-B’ lattice) and a third neighbour term ($2\hat{x}$ etc in the B-B’ lattice).

It is important we appreciate the various terms in the expression for $\mathcal{A}\{\mathbf{S}\}$ above. The ‘kernel’ $G_{ff0}^{-1}(\vec{r}_i - \vec{r}_j, i\omega_n)$ is specified by the $J = 0$ bandstructure of the B-B’ problem, explicit information about the spin variables is encoded in g_{ij} , and the fermions are defined *in the background* $\{\mathbf{S}\}$.

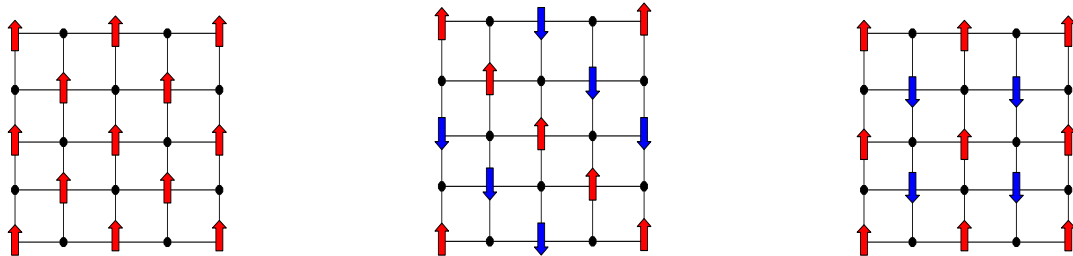


FIG. 1: Colour online: The three magnetic phases in the 2D model. Left: ferromagnetic (FM), center: antiferromagnet (AFM1), right: antiferromagnet (AFM2). These occur with increasing electron density. The moments are on the B sites, we have not shown the induced moments on the B' sites.

We define $i\nu_n = i(2n + 1)\pi$, so

$$A\{\mathbf{S}\} = \sum_{in} (i\nu_n + \beta\mu) \bar{\gamma}_{in} \gamma_{in} - \sum_{ijn} g_{ij} \frac{\beta^2 h_{ij}}{i\nu_n + \beta\mu - \Delta} \bar{\gamma}_{in} \gamma_{jn}$$

The internal energy can be calculated as $U\{\mathbf{S}\} = -\frac{\partial \ln Z}{\partial \beta} = -\langle \frac{\partial A\{\mathbf{S}\}}{\partial \beta} \rangle$. Simplifying the resulting expression and using the same principle as in DE we can write an explicit (but approximate) model purely in terms of core spins:

$$\begin{aligned} H_{eff}\{\mathbf{S}\} &= \sum_{ij} D_{ij} \sqrt{\frac{1 + \mathbf{S}_i \cdot \mathbf{S}_j}{2}} \\ D_{ij} &= h_{ij} \frac{1}{\beta} \sum_n B(i\omega_n) \langle e^{i\Phi_{ij}} \bar{\gamma}_{in} \gamma_{jn} \rangle + h.c \\ B(i\omega_n) &= \frac{(2i\omega_n + 2\mu - \Delta)}{(i\omega_n + \mu - \Delta)^2} \end{aligned} \quad (15)$$

The effective exchange D_{ij} can be determined at any temperature by the SCR method. The couplings take two values, D_1 for NN B-B exchange, and D_2 for second neighbour B-B exchange. The low T exchange can be estimated by evaluating the fermionic average in the perfectly spin-ordered state at $T = 0$ (after checking that the ground state generated by the exchange is self-consistently ferromagnetic). The evaluation of the Matsubara sums, *etc*, is discussed in Appendix A.

V. RESULTS

A. The magnetic ground state

Both ED-MC done on 8×8 , and TCA done on 16×16 exhibit the presence of three phases: namely ferromagnetic (FM, first panel in Fig.1), a 'line like' antiferromagnetic phase (AFM1, middle panel) and the more conventional antiferromagnet (AFM2) in the last panel. If we define the ordering wave-vector on B sublattice using axes along the diagonals, the FM phase has order at $\mathbf{Q} = \{0, 0\}$, AFM1 has order at $\mathbf{Q} = \{0, \pi\}$, and AFM2

has order at $\mathbf{Q} = \{\pi, \pi\}$. We could of course define the wave-vectors on the full B-B' lattice and use the usual x and y axes, but for the structurally ordered case the earlier convention is simpler.

Fig 2 shows the $n - T$ phase diagram for three values of Δ . With increasing n the phases occur in the sequence FM, AFM1, AFM2, AFM1 and FM again. The sequence as well as the rough filling windows are similar for all three Δ values (the VC, which is free of size effects, will demonstrate this more clearly). Fig 2(b) shows that for intermediate level difference, $\Delta = 4$, the T_c for the ferromagnetic phases actually increase a little bit. The T_c of the antiferromagnetic phases, however, decrease. Moreover, the $\{0, \pi\}$ phase is unobservable on the high filling side, while its Neel temperature, T_N , is quite small even on the low filling side. Eventually, for large enough Δ ,

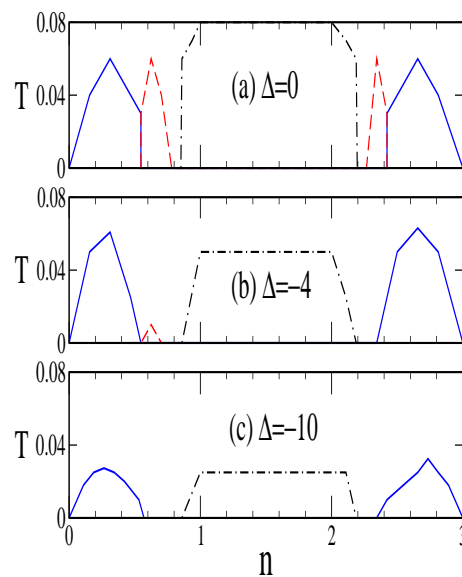


FIG. 2: Colour online: $n - T$ phase diagram based on TCA. (a) $\Delta = 0$, (b) $\Delta = -4$, and (c) $\Delta = -10$. The solid (blue) lines are ferro, dashed (red) lines are AFM1 and the dash-dot (black) lines are AFM2. The system size is 16×16 .

the T_c of even the ferromagnetic phases decrease, as seen in Fig 2(c). The AFM1 phase is unobservable on even the low filling side, possibly due to very small T_N .

While AFM phases driven by B-B superexchange have been studied in the DP's, AFM phases *driven by electron delocalisation* have not seen much discussion. Their occurrence, however, is not surprising. If we were to 'test out' the feasibility of various magnetic ground states we could restrict ourself to a few simple collinear phases to start with. The FM, AFM1, etc, are such examples. Let us index them by some index α . As described before, which of these occur at a chemical potential μ can be simply checked by calculating the energy $\mathcal{E}_\alpha(\mu) = \int_{-\infty}^{\mu} d\epsilon N_\alpha(\epsilon)\epsilon$, where $N_\alpha(\epsilon)$ is the electronic density of states in the spin background α . The phase appropriate to a particular μ would be the one with lowest energy. Even without a calculation it is obvious that the FM state will have the largest bandwidth, and would be preferred at low n . The AFM phases have narrower bands, but larger density of states (since the overall DOS is normalised), and with growing μ they become viable. In what follows we quantify this carefully.

One can obtain analytic expressions for the dispersions in the $\{0, \pi\}$ and $\{\pi, \pi\}$ phases, which are given below. In the $\{0, \pi\}$ phase, in our $J \rightarrow \infty$ limit, the structure decomposes into electronically decoupled ferromagnetic zigzag chains aligned antiferromagnetically with respect to each other, see Fig.1 middle panel. Their dispersion is 1D-like, given by:

$$\epsilon_{\mathbf{k}} = \frac{\Delta \pm \sqrt{\Delta^2 + 16 + 16\cos(k_x - k_y)}}{2} \quad (16)$$

In the limit $\Delta \rightarrow 0$, their 1D like nature is clearly visible:

$$\epsilon_{\mathbf{k}} = 2\sqrt{2}\cos\left(\frac{k_x - k_y}{2}\right) \quad (17)$$

The $\{\pi, \pi\}$ phase, on the other hand, decouples into two planar lattices where the B spins are arranged ferromagnetically, while these lattices are themselves aligned

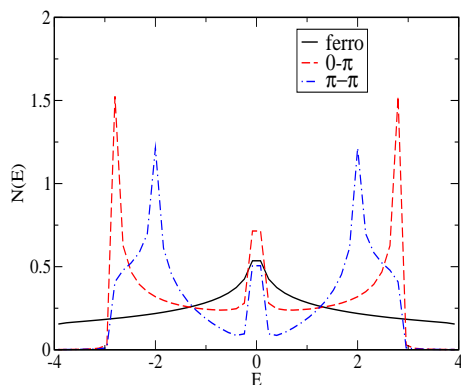


FIG. 3: Colour online: Electronic density of states for the three variational states, with $\mathbf{Q} = \{0, 0\}$, $\{0, \pi\}$ and $\{\pi, \pi\}$ at $\Delta = 0$

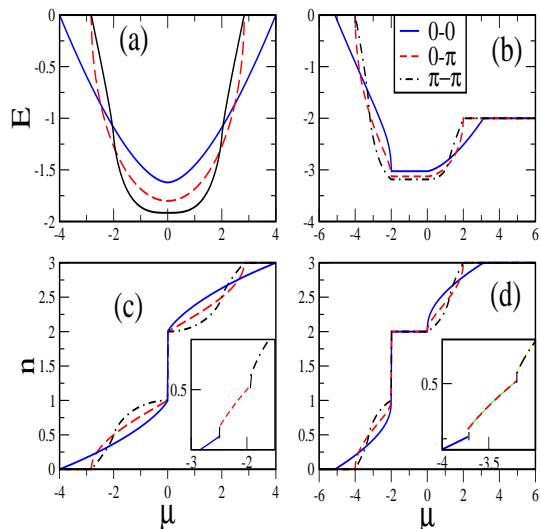


FIG. 4: Colour online: Electronic energy (top) and filling n (bottom) versus chemical potential for the three phases, $\Delta = 0$ (left), $\Delta = -2$ (right)

antiferromagnetically with respect to each other. The dispersion is given by:

$$\epsilon_{\mathbf{k}} = \frac{\Delta \pm \sqrt{\Delta^2 + 16t^2(\cos^2 k_x + \cos^2 k_y)}}{2} \quad (18)$$

which reduces to $\pm 2t\sqrt{\cos^2 k_x + \cos^2 k_y}$ when $\Delta = 0$. It is interesting to note that the bandwidths of both $\{0, \pi\}$ and $\{\pi, \pi\}$ phases are identical, although the detailed DOS are different. The DOS for the three phases for $\Delta = 0$ are shown in Fig 3. We can understand the occurrence of the various phases by integrating the DOS and comparing the energies at a fixed μ . The results are shown in Fig 4(a) for $\Delta = 0$ and Fig 4(b) for $\Delta = -2$.

As expected, at low filling the energy of the FM phase is the lowest, while for intermediate filling that of the AFM1 phase is lower than the FM phase. At still higher fillings, the energy of the AFM2 phase is the lowest. This is repeated symmetrically on the other side of $\mu = 0$ for $\Delta = 0$. The density discontinuity corresponding to each transition can also be found from the corresponding $\mu - n$ curves. For finite Δ , the AFM1 phase becomes narrower, especially on the high filling side. These simple variational results are corroborated by the phase diagram obtained from the TCA calculation.

The $n - \Delta$ phase diagram at $T = 0$ is shown in Fig 5. There are windows of phase separation (PS) where homogeneous electronic/magnetic states are not allowed. These regions correspond to the jumps in the $n - \mu$ curve. The AFM1 phase becomes unstable on the high filling side for large Δ , which manifests itself through a merging of the phase boundaries.

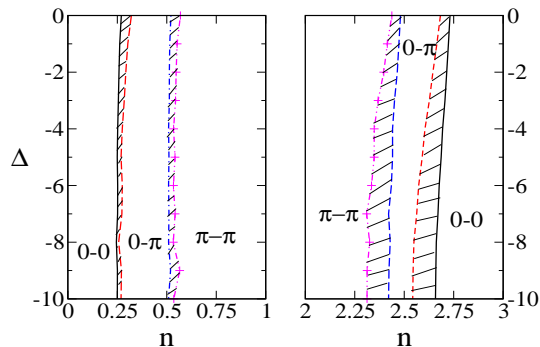


FIG. 5: Colour online: $n-\Delta$ phase diagram at $T = 0$ from the variational calculation. The hashed regions indicate windows of phase separation between the adjoining phases.

B. Spin model and effective exchange

Our effective spin model is:

$$H_{eff}\{\mathbf{S}\} = \sum_{ij} D_{ij} \sqrt{\frac{1 + \mathbf{S}_i \cdot \mathbf{S}_j}{2}}$$

Using the exchange D_{ij} calculated from Eq 15 using a fully ferromagnetic reference state, one can plot the nearest neighbour exchange D_{NN} and the next nearest neighbour D_{NNN} as a function of filling n . The results are shown in the top panel of Fig 6(a) for $\Delta = 0$. One finds that both the exchanges change sign as a function of filling. At low filling and very high filling, both are negative, indicating an overall ferromagnetic coupling. However, for intermediate values of filling, both the exchanges become positive, giving an effective antiferromagnetic coupling. In between, there is a small region where one of them is positive and the other negative.

Since the calculation was started using a purely ferromagnetic spin background, such changes in sign of the calculated exchange indicate an instability of the ferromagnetic phase at these fillings. Where the ‘exchange’ $D_{NN} + D_{NNN} > 0$ the ground state will no longer be FM, the result for D_{ij} is not self-consistent, and the quantitative values not trustworthy. We will confine ourselves to the window where the ground state is self consistently ferromagnetic.

The exchange for the antiferromagnetic states, and the Neel temperature, should be calculated in appropriate spin backgrounds, i.e., $\{0, \pi\}$ and $\{\pi, \pi\}$. However, the $\{0, \pi\}$ state, in the $J \rightarrow \infty$ case, consists of disconnected chain-like structures. While the intra-chain arrangement is ferromagnetic, the inter-chain arrangement is antiferromagnetic. Since there is no hopping connectivity between the chains, the inter-chain exchange calculated in such a spin background would emerge to be zero. Similarly, for a $\{\pi, \pi\}$ spin background, there are two sublattices such that the intra-sublattice arrangement is ferromagnetic, while the inter-sublattice one is anti-ferromagnetic. Again, since these sublattices are disconnected, the inter-sublattice hopping is zero. In these anisotropic states the

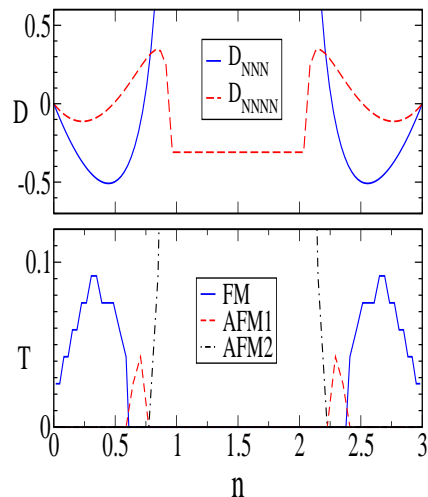


FIG. 6: Colour online: D_{ij} for NN and NNN, $\Delta = 0$ (top) and $n-T$ phase diagram obtained from a Monte Carlo using this exchange (bottom).

effective exchange (and stiffness) vanishes along certain directions at $T = 0$. To calculate the effective exchange that controls the T_c in the AFM1 and AFM2 phases we need to necessarily solve the finite temperature self-consistency problem. This is an interesting problem, but computationally demanding, and is left for future work.

C. $n-T$ phase diagram from the D_{ij}

Our previous experience with the double exchange model suggests²⁶ that a reasonable estimate of T_c is provided by the exchange calculated in the fully FM $T = 0$ state. On this assumption, one can study the effective spin model with classical Monte Carlo and calculate finite temperature properties including T_c . The $n-T$ phase diagram obtained this way is shown in the bottom panel of Fig 6. All the three phases: FM, AFM1, and AFM2 occur in approximately the correct filling windows. The T_c scales for the ferromagnetic phases, which are the only ones consistent with the assumed spin background, turn out to be reasonably correct, as we will see in a comparison with the full TCA result. We ignore the T_c for the AF phase since the AF exchange is not self-consistent.

D. Properties in the ferromagnetic regime

Since much of the interest in the double perovskites arises from ferromagnetism, we focus on this regime in what follows. In our $n-T$ phase diagram, this FM phase at low filling occurs upto $n \approx 0.5 - 0.7$. From the variational calculation, which is essentially in the ‘bulk limit’, the FM window is upto $\sim 0.3 - 0.4$. Considering the degeneracy of the three t_{2g} orbitals, translates to about 0.9 – 1.2 electrons per unit cell. $\text{Sr}_2\text{FeMoO}_6$, which has

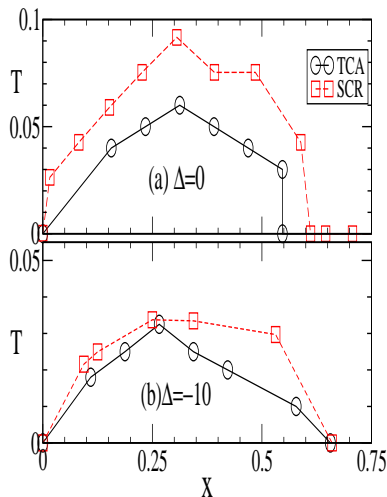


FIG. 7: Colour online: Ferromagnetic part of the phase diagram for low ‘filling’¹⁷, $x = 3 - n$, compared between TCA and SCR, for (a) $\Delta = 0$, (b) $\Delta = -10$ both calculated for size 16×16

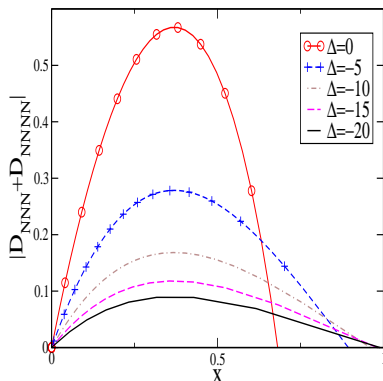


FIG. 8: Colour online: Effective exchange in the ferro phase $|D_{NNN} + D_{NNNN}|$ for different Δ , obtained from SCR. The exchange calculation is on a k grid 1000×1000 , and the filling¹⁷ is $x = 3 - n$.

one electron per unit cell, falls within this regime. However, many other materials like $\text{Sr}_2\text{FeReO}_6$ are known, which have 2 or more electrons per unit cell, but are still ferromagnetic with a high T_c . This discrepancy between theory and experiment was noticed by many authors before us: Chattopadhyay and Millis¹³, L.Brey *et. al.*²⁰, E. Carvajal *et.al.*¹⁵ and J.L.Alonso *et. al.*¹⁶. They attributed it to the presence of competing antiferromagnetic channels, an effect which we also find.

Our results on $T_c(n)$ is similar to that obtained by others, *i.e.*, a reduction as $n \rightarrow 0$ as the kinetic energy and ferromagnetic exchange weakens, and a drop also at large n due to the presence of competing AF phases. The $T_c(n)$ obtained from the SCR scheme is compared to the result of full spin-fermion Monte Carlo using TCA, Fig 7. They seem to match quite well, except that the SCR results calculated on a $T = 0$ state overestimate the T_c slightly.

While the actual T_c -s can only be calculated using Monte Carlo on small systems, eg. for 16×16 in Fig 7, the average exchange can be calculated with a very large k grid (1000×1000 k points). This $T = 0$ exchange, based on an assumed FM state has the behaviour shown¹⁷ in Fig 8. While this result has a clear correspondence with the $T_c(n, \Delta)$ results obtained from DMFT by Millis *et. al.*, and the calculations of Carvajal *et.al.*, it overestimates the window of FM, and misses the first order FM to AFM transition. The actual $T_c(x)$ will have a discontinuity with increasing x , instead of decreasing smoothly to zero.

E. The AFM phases

The AFM phases AFM1 and AFM2 occupy a large part of the $n - T$ phase diagram. The presence of such collinear antiferromagnetic phases have been observed earlier by several authors, notably Alonso *et.al.*¹⁶. These phases, at least within the $J \rightarrow \infty$ model considered here, have a ‘lower connectedness’ than the ferromagnetic phase. The AFM1 phase consists of double staircase-like structures attached back to back, while the AFM2 phase consists of decoupled Cu-O like lattices for each B’ spin channel. The DOS corresponding to these are given in Fig 3. The DOS for the AFM1 phase resembles that of a 1D tightbinding lattice, while the AFM2 DOS is more 2D-like. It is interesting to note that there is a dispersionless level for both the AFM phases, which gives the jump in the $\mu - n$ curve. While the effective exchange calculation starting from a fully polarized background already produced the three phases, but a truly self-consistent calculation for the AFM phases would have to start assuming these spin backgrounds. Such a calculation is non-trivial, as discussed before.

VI. MAGNETISATION AT THE B’ SITES

The induced magnetism on the B’ site was explained within a local ‘level repulsion’ picture by Sarma *et al.*¹², but a lattice-oriented approach is lacking. Some headway can be made by exactly integrating out the B degrees of freedom rather than the B’ from the $J \rightarrow \infty$ model given in Eq 2, but the result is in the form of an action, rather than an effective Hamiltonian. Within second order perturbation theory, however, it appears that an extra onsite term of the form $\frac{zt_{FM}^2}{2\Delta} \sum_{j\delta\alpha\beta} \vec{S}_{j+\delta} \cdot m_{j\alpha}^\dagger \vec{\sigma}_{\alpha\beta} m_{j\beta}$ occurs for the B’ sites (z is the number of nearest neighbours) giving an ‘exchange splitting’ at the B’ site, with the spins of the surrounding B sites serving as a magnetic field. The corresponding hopping terms are given by:

$$\begin{aligned} & \frac{t_{FM}^2}{\Delta} \sum_{\langle ij \rangle, \sigma} (m_{i\sigma}^\dagger m_{j\sigma} + \frac{t_{FM}^2}{\Delta} \sum_{\langle ij \rangle} \vec{S}_{i+\delta} \cdot m_{i\alpha}^\dagger \vec{\sigma}_{\alpha\beta} m_{j\beta} \\ & + \frac{t^2}{2\Delta} \sum_{\langle\langle ij \rangle\rangle} \vec{S}_{(i-j)/2} \cdot m_{i\alpha}^\dagger \sigma_{\alpha\beta} m_{j\beta} \end{aligned} \quad (19)$$

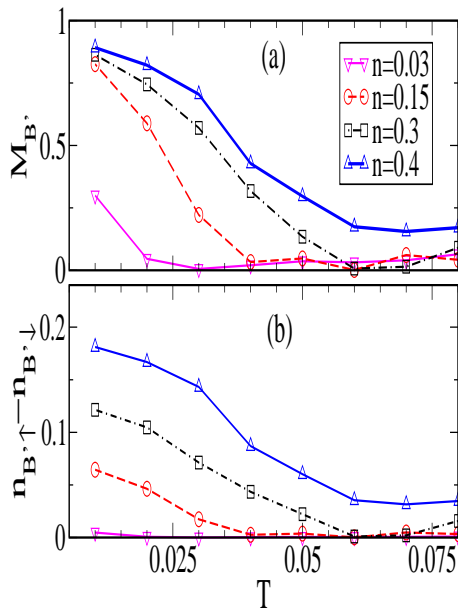


FIG. 9: Colour online: Temperature dependence of B' site magnetization for different filling, from ED-MC on a 8×8 system at $\Delta = 0$. The top panel plots the magnetisation normalized by the total B' occupancy, while the bottom panel shows the unnormalized magnetisation.

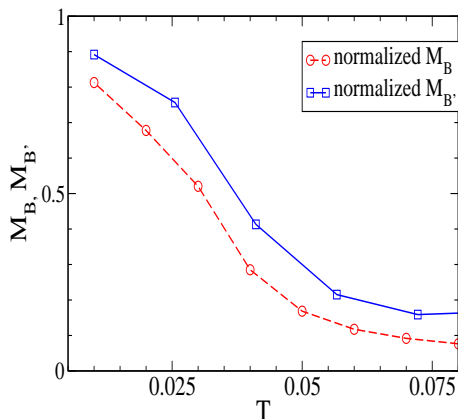


FIG. 10: Colour online: Comparison of the electronic magnetisation at the B' site with the core spin magnetization at the B site. The result is for $n = 0.4$ using ED-MC on a 8×8 system. Both the B and B' results are normalised to highlight their similar temperature dependence.

Within a mean-field treatment of the B core spins $\mathbf{S}_i \approx \langle \mathbf{S}_i \rangle = \hat{z}M$, the effective B'-B' 'hamiltonian' can be written as:

$$\begin{aligned}
 & \frac{t^2}{\Delta} \sum_{\langle ij \rangle} [(1+M)m_{i\uparrow}^\dagger m_{j\uparrow} + (1-M)m_{i\downarrow}^\dagger m_{j\downarrow}] \\
 & + \frac{t^2}{2\Delta} \sum_{\langle\langle ij \rangle\rangle} [(1+M)m_{i\uparrow}^\dagger m_{j\uparrow} + (1-M)m_{i\downarrow}^\dagger m_{j\downarrow}] \\
 & + \frac{2t^2}{\Delta} M \sum_i (m_{i\uparrow}^\dagger m_{i\uparrow} - m_{i\downarrow}^\dagger m_{i\downarrow})
 \end{aligned} \quad (20)$$

Obviously, at $T = 0$, $M = 1$, and only one spin species hops.

The effective spin polarization at the B' site, which is purely electronic, contributes to the total magnetization. Within the TCA approach using the Hamiltonian 2, this can simply be estimated by calculating the normalized magnetization $\frac{\langle n_{\uparrow}^{B'} \rangle - \langle n_{\downarrow}^{B'} \rangle}{\langle n_{\uparrow}^{B'} \rangle + \langle n_{\downarrow}^{B'} \rangle}$. In Fig 9(a), the magnetization of the B' has been plotted against the temperature for different fillings corresponding to an ED-MC simulation on a 8×8 system for $\Delta = 0$, normalized by the net B' filling. It is observed that the T dependence is very similar to that the B core spin case. In Fig 9(b), the bare B' magnetization is shown without normalization: it shows that the saturation magnetization increases with filling, as expected. In Fig 10, a comparison of the M vs T coming from the B' electron and the B core spins is provided.

VII. THE EFFECT OF B'-B' HOPPING

Inclusion of B'-B' hopping t' would result in the same expression for the exchange calculated in the ferromagnetic state as before (see Appendix A), except that the Δ everywhere would get replaced by $\Delta + 4t' \cos k_x \cos k_y$, while $\epsilon_{\mathbf{k}} = 2t(\cos k_x + \cos k_y)$ for a square lattice. It is obvious that if $t = 0$, the exchange would vanish irrespective of t' , showing that hopping across the magnetic site is crucial, as expected. For parameter values reasonable in double perovskites, $t' \approx 0.1 - 0.3t$, and $0 \leq \Delta < 3$, there is almost no change in the $n - \Delta$ phase diagram, although the T_c values decrease marginally when the t' is turned on. For larger values of Δ , the AFM1 phase becomes unstable, and the ferromagnetic window extends a bit, upto the AFM2 phase, although the T_c s, of course, are proportionately low.

VIII. DISCUSSION

We discuss a few issues below to connect our results to available data on the double perovskites, and also highlight a few effects that we have neglected.

1. *Material parameters:* Ab initio calculations suggest^{12,13} that $t \sim 0.3 - 0.5\text{eV}$, while t' is typically 3-5 times smaller. The direct hopping between B sites is even smaller, $\sim 0.05\text{eV}$. Estimates for the bare 'charge transfer gap' Δ (in SFMO) vary between 1.4eV ¹² to about 2eV ¹³. Hence, the parameter window we explored seems reasonable. Our ferromagnetic T_c are typically $0.1t$ at a filling appropriate to SFMO, so the absolute magnitude of the T_c -s would be about $360 - 600\text{K}$, roughly the range seen in the for double perovskites.

2. *B-B hopping:* While we have not considered the effect of B-B hopping, the smallest energy scale in the problem, explicitly in this paper, it is possible to understand qualitatively the effect of including this hopping. If only B-B' hopping is considered, then there are two

singular features in the density of states, at ϵ_B and $\epsilon_{B'}$, or alternatively, at 0 and $\tilde{\Delta}$. Inclusion of the B'-B' hopping resulted, at the zeroth level, in the smoothening of the feature at $\epsilon_{B'}$. Similarly, inclusion of the B-B hopping will basically smoothen out the feature at ϵ_B . However, the B'-B' hopping had a much more dramatic consequence in terms of providing an alternate pathway for delocalization of the B' electrons irrespective of spin, especially at large Δ . Secondly, it resulted in connecting up of the AFM1 staircases, getting rid of their 1D character, and making this phase unstable compared to the FM and AFM2 phases. Inclusion of a small B-B hopping in addition, is not, on the other hand, expected to have any more dramatic consequences. We can readily include this in our formalism.

3. *Three dimensions:* The entire analysis in this paper was in two dimensions. Apart from simplicity, ease of visualization, and computational tractability, there is a definite argument in terms of the symmetry of the t_{2g} orbitals as long as nearest neighbour interactions are considered^{13,15}, which says that one can consider three independent 2D Hamiltonians. Other authors^{21,23} have also used 2D Hamiltonians. Having said that, the phases discussed here generalizes easily to three dimensions. The AFM1 phase in the absence of B'-B' hopping becomes 2D rather than 1D, consisting of ferromagnetic [111] planes arranged antiferromagnetically. Such an arrangement has been observed by authors like Alonso *et. al.*¹⁶, and even in *ab initio* calculations²².

4. *Filling control:* The $n - T$ phase diagram that we provide is for a definite set of parameters Δ, t, t' etc. While going across the series of DP compounds $\text{Sr}_2\text{FeMoO}_6$, to $\text{Sr}_2\text{FeReO}_6$, it is not just the filling but also all these parameters which are changing. A more controlled way of varying the filling alone would probably be to dope the compounds at the A site, namely prepare the series $\text{Sr}_{2-x}\text{La}_x\text{FeMoO}_6$. While some work has been done in this regard²⁴, more extensive work, probing higher doping values is necessary to ascertain whether such antiferromagnetic phases are indeed observed.

5. *SCR for antisite disordered case:* While the clean problem has been studied in detail in this paper, antisite disorder is expected to make it more interesting. Paradoxical effects like increase in T_c and widening of the FM region has been suggested¹⁶. The scheme for self-consistent renormalization that we have proposed can be generalized even to the case of antisite disorder (see Appendix). However, the scheme in that case becomes more numerical, and the analytical handle available here would be lost even at $T = 0$. The formalism is presented in the Appendix and we are currently studying the problem.

IX. CONCLUSION

We have suggested a scheme for extracting a simple magnetic model for double perovskites starting with a tight binding parametrisation of the electronic structure.

The 'exchange scale' in this model is related to the electronic kinetic energy. The ferromagnetic T_c estimated from this exchange compares well with results from the full spin-fermion Monte Carlo. The change in sign of the exchange with increasing carrier density captures the phase competition in the electronic model and the transition in the magnetic ground. Our scheme, extended to include multiple bands and spin-orbit coupling would allow a controlled and economical approach to the finite temperature physics of a wide variety of double perovskites. Another fruitful line of exploration is to include antisite disorder. We have highlighted the scheme in the appendix and hope to present results in the near future.

We acknowledge discussions with D. D. Sarma, Brijesh Kumar and Rajarshi Tiwari, and use of the Beowulf cluster at HRI.

X. APPENDIX A: EXCHANGE CALCULATION IN THE DOUBLE PEROVSKITES

The effective exchange D_{ij} can be evaluated in the perfectly spin-ordered state at $T=0$. This can be obtained by using the known form of the Green's function $\langle \bar{\gamma}_{in} \gamma_{jn} \rangle$ at $T=0$, namely it is the $G_{ff0}(\vec{r}_i - \vec{r}_j, i\omega_n)$ obtained before, made dimensionless by dividing by β . Hence, in the spin ordered case, the exchange becomes:

$$U_B(T=0) = \frac{1}{\beta} \sum_n \frac{(2i\omega_n - \Delta)}{(i\omega_n - \Delta)^2} \frac{\epsilon_k^2}{\left[i\omega_n - \frac{\epsilon_k^2}{i\omega_n - \Delta} \right]}$$

$$= \frac{1}{\beta} \sum_n \frac{(2i\omega_n - \Delta)\epsilon_k^2}{(i\omega_n - \Delta)[i\omega_n(i\omega_n - \Delta) - \epsilon_k^2]} \quad (21)$$

Expanding in partial fractions, this can be written as:

$$U_B = \frac{1}{\beta} \sum_{kn} \left[\frac{E_{k+}}{i\omega_n - E_{k+}} + \frac{E_{k+}}{i\omega_n - E_{k-}} - \frac{\Delta}{i\omega_n - \Delta} \right] \quad (22)$$

Performing the Matsubara sums, this gives the final result

$$U_B = \sum_k [E_{k+} n_F(E_{k+}) + E_{k-} n_F(E_{k-})] - \Delta n_F(\Delta) \quad (23)$$

The last term is an additional contribution obtained from the missing B' energy. While this gives the full internal energy in the spin polarised case, the bond-resolved exchange D_{ij} is given by

$$D_{ij} = \sum_k e^{i\vec{k} \cdot (\vec{r}_i - \vec{r}_j)} [E_{k+} n_F(E_{k+}) + E_{k-} n_F(E_{k-}) - \Delta n_F(\Delta)] \quad (24)$$

We need to do the k-sum, which can only be done numerically for square (2D) or cubic (3D) lattices. Instead, if one uses a Bethe lattice of infinite coordination,

then the bare density of states for nearest neighbour hopping is semicircular, and analytic treatment is possible, at least for the DOS. In our case, there are two bands, with dispersions

$$E_{k\pm} = \frac{\Delta \pm \sqrt{\Delta^2 + 4\epsilon_k^2}}{2} \quad (25)$$

The density of states for these bands is:

$$\begin{aligned} \rho_{\pm}(E) &= \sum_k \delta\left(E - \frac{\Delta \pm \sqrt{\Delta^2 + 4\epsilon_k^2}}{2}\right) \\ &= \int d\omega \rho_0(\omega) \delta\left(E - \frac{\Delta \pm \sqrt{\Delta^2 + 4\omega^2}}{2}\right) \end{aligned} \quad (26)$$

where the bare DOS $\rho_0(\omega) = \sum_k \delta(\omega - \epsilon_k)$ is approximated by the semicircular DOS, $\rho_0(\omega) \approx \frac{2}{\pi D^2} \sqrt{D^2 - \omega^2}$. Then, the full DOS given by Eq 26 becomes:

$$\rho_{\pm}(E) = \frac{2}{\pi D^2} \int_{-D}^D d\omega \sqrt{D^2 - \omega^2} \delta\left(E - \frac{\Delta \pm \sqrt{\Delta^2 + 4\omega^2}}{2}\right) \quad (27)$$

This integral can be evaluated, to give the following analytic result for the DOS:

$$\begin{aligned} \rho_{\pm}(E) &= \frac{\pm(2E - \Delta) \sqrt{D^2 - E^2 + E\Delta}}{\pi D^2 \sqrt{E^2 - E\Delta}} \\ &\times \Theta(D^2 - E^2 - E\Delta) \Theta(E^2 - E\Delta) \end{aligned} \quad (28)$$

Obviously, this diverges at $E = 0$, and $E = \Delta$. The limits of the DOS, and hence the integral, are obtained from the equations given by the two theta function conditions: $E_{limit}^{(1)} = \frac{\Delta + \sqrt{\Delta^2 + 4D^2}}{2}$, $E_{limit}^{(2)} = 0$, Δ . If we take $\Delta < 0$, as in our case, then the lower band lies between $\frac{\Delta + \sqrt{\Delta^2 + 4D^2}}{2}$ (left edge) and Δ (right edge), while the upper band lies between 0 (left edge) and $\frac{\Delta - \sqrt{\Delta^2 + 4D^2}}{2}$ (right edge).

When $D \rightarrow 0$, i.e., $t \rightarrow 0$, the theta function conditions are only satisfied together for $E^2 - E\Delta = 0$, i.e., at $E = 0$ or $E = \Delta$. Thus we recover the bare levels as δ -function peaks in the DOS, as expected.

The exchange at $T=0$ is given in terms of this DOS as:

$$U_B = \int E[\rho_+(E) + \rho_-(E)]n_F(E)dE - \Delta n_F(\Delta) \quad (29)$$

This gives U_B as a function of μ . One can also obtain the total number of electrons N from the DOS as a function of μ :

$$N = \int dE[\rho_+(E) + \rho_-(E)]n_F(E) \quad (30)$$

From Eq 29 and Eq 30, eliminating μ , one can get U vs N .

Using the substitution $\omega = E^2 - E\Delta$, the expression for the exchange can be rewritten in a more convenient form at $T=0$ as:

$$\begin{aligned} U_B(\mu) &= \frac{2}{\pi D^2} \sum_{\pm} \int_{-D}^D d\omega \frac{\Delta \pm \sqrt{\Delta^2 + 4\omega^2}}{2} \\ &\times \Theta\left(\mu - \frac{\Delta \pm \sqrt{\Delta^2 + 4\omega^2}}{2}\right) \sqrt{D^2 - \omega^2} \\ &- \Delta \Theta(\mu - \Delta) \end{aligned} \quad (31)$$

It is to be noticed that as $t \rightarrow 0$, i.e., $D \rightarrow 0$, the exchange goes to zero, as it should. This can be seen in two ways. Firstly, as $t \rightarrow 0$, $\epsilon_k \rightarrow 0$. Hence, the band dispersions $E_{k\pm}$ given by Eq 25 tends to $\frac{\Delta \pm |\Delta|}{2}$. This means that $E_{k+} \rightarrow 0$ and $E_{k-} \rightarrow \Delta$. Hence, putting in Eq 29, the first term involving E_{k+} is 0, while the second term involving E_{k-} cancels the third term involving $\Delta n_F(\Delta)$.

The other way to observe this is to use Eq 31. Here, when $D \rightarrow 0$, then the theta function condition is only satisfied for $\omega^2 = D^2$, which means that the only contribution to the integral comes from $\omega = 0$. Indeed, the bare semicircular DOS $\frac{2}{\pi D^2} \sqrt{D^2 - \omega^2}$ being a normalized object, tends to a delta function $\delta(E)$ as $D \rightarrow 0$. Hence, the term involving $+$ sign gives 0, while that involving $-$ sign gives $\Delta \Theta(\mu - \Delta)$, which cancels with the third term.

XI. APPENDIX B: EXCHANGE CALCULATION WITH ANTISITE DISORDER

Firstly, the Hamiltonian has to be written in such a way that all the B and B' degrees of freedom are separated out in distinct subspaces of the Hamiltonian.

$$H = \begin{pmatrix} H_{FF} & H_{FM} \\ H_{MF} & H_{MM} \end{pmatrix}$$

where H_{FF} represents the terms in the subspace of the B degrees of freedom, while H_{MM} represents the terms in the B' subspace. H_{MF} and H_{FM} connects the two subspaces.

The B Green's function satisfies the matrix equation

$$G_{FF}^{-1}(i\omega_n) = i\omega_n \mathbf{I} - H_{FF} - H_{FM}(i\omega_n \mathbf{I} - H_{MM})^{-1} H_{MF} \quad (32)$$

Written out term by term,

$$G_{FF}^{-1}(i\omega_n) = i\omega_n \delta_{ij} - H_{FF_{ij}} - \sum_{kl} H_{FM_{ik}} (i\omega_n \mathbf{I} - H_{MM})_{kl}^{-1} H_{MF_{ij}} \quad (33)$$

Hence the action

$$\begin{aligned} \mathcal{A}\{S\} &= \sum_{in} (i\nu_n + \beta\mu) \bar{\gamma}_{in} \gamma_{in} - \sum_{ij} \beta H_{FF_{ij}} \bar{\gamma}_{in} \gamma_{jn} g_{ij} \\ &- \beta^2 \sum_{kl} H_{FM_{ik}} (i\nu_n \mathbf{I} - \beta H_{MM})_{kl}^{-1} H_{MF_{ij}} \bar{\gamma}_{in} \gamma_{jn} g_{ij} \end{aligned}$$

Now, let V be the diagonalizing matrix of H_{MM} and its eigenvalues are λ_{MM}^p . Then,

$$\mathcal{A}\{S\} = \sum_{in} (i\nu_n + \beta\mu)\bar{\gamma}_{in}\gamma_{in} - \sum_{ijn} [\beta H_{FFij} - \beta^2 \sum_{klp} \frac{H_{FMik} V_{kp} V_{pl}^{-1} H_{MFij}}{i\nu_n - \beta\lambda_{MM}^p}] g_{ij} \bar{\gamma}_{in} \gamma_{jn}$$

$$\left\langle \frac{\partial \mathcal{A}}{\partial \beta} \right\rangle = \sum_{ij} \left[H_{FFij} - \sum_{klp} \frac{H_{FMik} V_{kp} V_{pl}^{-1} H_{MFij}}{i\nu_n - \beta\lambda_{MM}^p} + \beta^2 \sum_{klp} \frac{H_{FMik} V_{kp} \lambda_{MM}^p V_{pl}^{-1} H_{MFij}}{(i\nu_n - \beta\lambda_{MM}^p)^2} \right] g_{ij} \langle \bar{\gamma}_{in} \gamma_{jn} \rangle$$

$$= - \sum_{ij} D_{ij} g_{ij}$$

It is to be noted that in the ordered case, the hamiltonian matrix becomes block diagonal in k -space, and the elements of the off-diagonal block H_{MF} and H_{FM} are simply ϵ_k , while those of the diagonalizing matrices V are $e^{i\vec{k}\cdot(\vec{r}_i - \vec{r}_j)}$, while the eigenvalues λ_{MM}^p are simply ϵ_{M0} , i.e., Δ . Hence, the quantity $H_{FMik} V_{kp} V_{pl}^{-1} H_{MFij}$ in the numerator simply goes over to h_{ij} , as defined in Eq 15

-
- ¹ D.D. Sarma, Current Op. Solid St. Mat. Sci., **5**, 261 (2001).
² J. B. Philipp, P. Majewski, L. Alff, A. Erb, R. Gross, T. Graf, M. S. Brandt, J. Simon, T. Walther, W. Mader, D. Topwal, and D. D. Sarma, Phys. Rev. B, **68**, 144431.
³ B. Garcia Landa *et al*, Solid State Comm., **110**, 435 (1999).
⁴ B. Martinez, J. Navarro, L. Balcells and J. Fontcuberta, J. Phys.: Condens. Matter **12**, 10515 (2000).
⁵ D. D. Sarma, S. Ray, K. Tanaka, M. Kobayashi, A. Fujimori, P. Sanyal, H.R. Krishnamurthy and C. Dasgupta, Phys. Rev. Lett., **98**, 157205 (2007).
⁶ P. Sanyal, S. Tarat and P. Majumdar, Eur. Phys. J. **B 65**, 39, (2008).
⁷ S. Ray, A. Kumar, S. Majumdar, E.V. Sampathkumaran, D.D. Sarma, J. Phys.: Condens. Matter **13**, 607 (2001).
⁸ K.-I. Kobayashi, T. Okuda, Y. Tomioka, T. Kimura and Y. Tokura, J. Magn. Magn. Mat., **218**, 17 (2000).
⁹ K.W. Lee and W.E. Pickett, Phys. Rev. B, **77**, 115101 (2008).
¹⁰ Y. Kronenberger, K. Mogare, M. Reehuis, M. Tovar, M. Jansen, G. Vaitheeswaran, V. Kanachana, E. Bultmark, A. Delin, F. Wilhelm, A. Winkler and L. Alff, Phys. Rev. B, **75**, 020404 (R) (2007).
¹¹ G. Vaitheeswaran, V. Kanchana, A. Delin, Journal of Physics, Conference Series, **29**, 50 (2006).
¹² D.D. Sarma, P. Mahadevan, T. Saha Dasgupta, S. Ray, A. Kumar, Phys. Rev. Lett., **85**, 2549 (2000).
¹³ A. Chattopadhyay and A. J. Millis, Phys. Rev. B, **64**, 024424 (2001).
¹⁴ In this paper we will refer to this state as a *ferromagnetic* state, considering the order of the core spins.
¹⁵ E. Carvajal, O. Navarro, R. Allub, M. Avignon and B. Alascio, Eur. Phys. J. B, **48**, 179-187 (2005).
¹⁶ J.L. Alonso, L.A. Fernandez, F. Guinea, F. Lesmes, and V. Martin-Mayor, Phys. Rev. B, **67**, 214423 (2003).
¹⁷ The x -axis represents $(3-n)$ rather than n . This is done to avoid numerical problems associated with the calculation of the exchange on the low filling side due to the singularity at $\mu = \Delta$. For small Δ , of course, there is an explicit symmetry between the two sides, but for larger Δ , the ferromagnetic phase seems to have a larger extent on the high filling side compared to the low filling one.
¹⁸ O.K. Andersen *et. al.*, in Tight-binding approach to Computational Materials Science, edited by L. Colombo, A. Gonis, and P. Turchi, MRS Symposia Proceedings No. 491 (Materials Research Society, Pittsburgh, 1998), pp3-34; O.K. Anderson *et. al*, cond-mat/9907064.
¹⁹ O.K. Andersen and T. Saha Dasgupta, Phys. Rev. B, **62**, R 16219, (2000).
²⁰ L. Brey, M.J. Calderon, S. Das Sarma, F. Guinea, Phys. Rev. B, **74**, 094429 (2006).
²¹ A. Taraphder and F. Guinea, Phys. Rev. B, **70**, 224438 (2004).
²² T.K. Mandal, C. Felser, M. Greenblatt, J. Kubler, *arXiv:0807.4689*.
²³ O. Navarro, E. Carvajal, B. Aguilar, M. Avignon, Physica B, **384**, (2006).
²⁴ D. Serrate, J.M.D. Teresa, J. Blasco, M.R. Ibarra, L. Morellon, Appl. Phys. Lett., **80**, 4573 (2002).
²⁵ S. Kumar and P. Majumdar, Eur. Phys. J. **B 50**, 571 (2006).
²⁶ S. Kumar and P. Majumdar, Eur. Phys. J. **B 46**, 315 (2005).